



Modeling for Control of a Wobble–Yoke Stirling Engine

Eloísa García–Canseco[§], Jacquelin M.A. Scherpen[†] and Marnix Kuindersma[†]

[§]Eindhoven University of Technology, Faculty of Mechanical Engineering, CST,
 PO Box 513, 5600 MB Eindhoven, The Netherlands.

[†]University of Groningen, Faculty of Mathematics and Natural Sciences
 ITM, Nijenborgh 4, 9747 AG Groningen, The Netherlands.

Email: e.garcia.canseco@tue.nl, j.m.a.scherpen@rug.nl

Abstract—In this paper we derive the dynamic model of a four–cylinder double–acting wobble–yoke Stirling engine introduced originally by [1, 2]. In contrast with the classical thermodynamics methods that dominate the literature of Stirling mechanisms, we present a control system perspective to obtain a useful model for the analysis and synthesis of feedback control laws. The main motivation is the application of this gas engine in a micro–combined heat and power (CHP) generation system.

Keywords: control, micro–CHP, modeling, Stirling engine, cogeneration system.

Nomenclature

a_i	connecting rod bearing center,
A_p	piston area [m ²]
A_r	piston rod area [m ²]
b_i	wobble yoke–beam bearing center,
b_{p_i}	damping coefficient,
c_j	nutating bearing center,
d	crankshaft bearing center,
e_n	axes of the fixed reference frame,
$F_{(\cdot)}$	force [N],
g	acceleration due to gravity [m/s ²],
I	mass moment of inertia about the pivot O [kgm ²],
k_{p_i}	piston spring constant [N/m],
$l_{(\cdot)}$	distance [m],
m	piston assembly mass including the connecting rod [kg],
m_T	total mass of the working gas [kg],
M_i	angular momentum with respect to the axis e_i [Nm],
O	center of the fixed reference frame, main pivot center,
p_{c_i}	pressure in compression space [N/m ²],
p_{cc}	crankcase pressure [N/m ²],
p_{e_i}	pressure in expansion space [N/m ²],
R	gas constant [J/(K · mol)],
T_h	hot end temperature [K],
T_k	cold end temperature [K],
T_r	regenerator effective temperature [K],
V_{c_i}	compression space volume [m ³],
V_{e_i}	expansion space volume [m ³],
V_{dc}	dead volume in compression space [m ³],
V_{de}	dead volume in expansion space [m ³],
V_h	heater volume [m ³],
V_k	cooler volume [m ³],
V_{swc}	swept volume in compression space [m ³],
V_{swe}	swept volume in expansion space [m ³],
z_i	vertical displacement [m],
$z_{i_{eq}}$	equilibrium length of the i -th piston spring [m],
$z_{i_{max}}$	maximum piston displacement= $h_s/2$ [m],
\dot{z}_i	velocity [m/s],
\ddot{z}_i	acceleration [m/s ²],

θ_j	beam angle [rad],
$\dot{\theta}_j$	beam angular velocity [rad/s],
$\ddot{\theta}_j$	beam angular acceleration [rad/s ²],
$\theta_{j_{max}}$	maximum beam angle [rad],
ϕ	crankshaft angle [rad],
τ	shaft torque [Nm].

1. Introduction

In the recent decades, there has been an enormous interest in the application of heat engines for conversion of different forms of heat source into electrical energy [3]. One of the most promising applications is the micro–combined heat and power (CHP) generation, or in other words, the simultaneous production of heat and power at a small–scale [4]. A micro–CHP consist of a gas engine which drives an electrical generator. The main purpose of a micro–CHP system is to replace the conventional boiler in a central heating system. Among the technologies that have been proposed for micro–CHP applications we can mention fuel cells, internal combustion engines and Stirling engines [4, 5].

Since the invention of the first Stirling engine by Robert Stirling in 1816, Stirling engines have been heavily studied, with an increasing interest during the last decades. Nevertheless, most of the studies rely on thermodynamics methods and intuitive design techniques. There exist few literature on the application of dynamics and control methods to investigate their stability and dynamic properties, see for instance [6–9] and the recent work [10]. Moreover, most of the works analyze free–piston Stirling engines.

In this work, we focus on the Whispergen micro–CHP with Stirling engine technology. This micro–CHP unit, developed by WhisperTech Limited [11], was originally designed as a battery charger for marine applications [1]. In contrast with most Stirling engines based on free–piston mechanisms, the Whispergen micro–CHP unit comprises a wobble–yoke mechanism with a four–cylinder double–acting engine configuration.

To the best of the authors knowledge, none of the previous works, namely [1, 2], have approached the study of the wobble–yoke Stirling engine from a control system perspective. Our main contribution is the development of a dynamic model of the wobble–yoke Stirling engine, that can be useful for the analysis and synthesis of feedback control laws for micro–CHP systems.

2. Description of the System

Figure 1 shows the schematic representation of the four–cylinder double–acting Stirling engine. The four cylinders

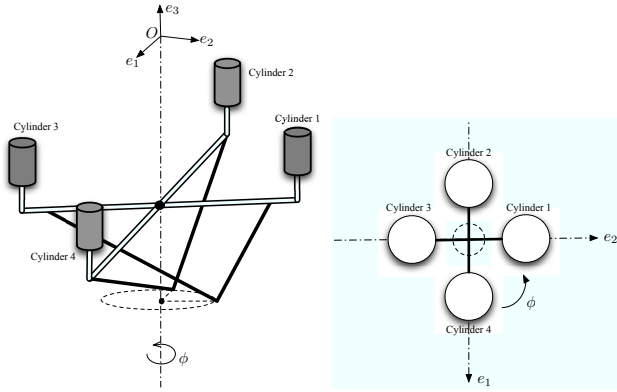


Figure 1: Schematic representation and cylinders configuration of the wobble yoke Stirling engine.

are phased at 90° from each other with respect to ϕ . The links connecting the cylinders sketch the wobble-yoke mechanism whose function is to translate the vertical motion of the cylinders into the rotational motion through the shaft angle ϕ . The wobble yoke drive is based on the well-known spherical crank-rocker four-bar linkage [12, 13]. Its working principle can be explained by reference to Figure 2. The mechanism is based on a beam which pivots about its center O in one plane (e_2e_3 for beam 1, and e_1e_3 for beam 2). Each beam is attached to the cylinders with connecting rods at each end via bearings a_1 and a_3 . An eccentric bearing c_1 is attached to the drive shaft and it is connected to the beam via two bearings b_1 and b_3 . The eccentric bearing c_1 is the rotating part of the mechanism. When the engine is working, the vertical motion of the pistons inside the cylinders, induces a rotational movement on bearing c_1 . Due to the geometrical and physical configuration of the mechanism, bearing c_1 describes a circle of radius l_{c_1d} . The axis of bearings b_1 , b_3 , c_1 and d must intersect the center O , so that the kinematic constraints of the spherical crank rocker are satisfied [12, 13]. An analogous discussion applies to the second beam. We refer the reader to [1, 2] for more details about the wobble-yoke Stirling engine.

3. Modeling for control

In this section we derive the equations of motion for the wobble-yoke Stirling engine depicted in Figure 1. We make the following fundamental Assumption throughout the work:

- a1 *Small motion*: Let $-15^\circ < \theta_i < 15^\circ$, then $\cos \theta_j \approx 1$, $\sin \theta_j \approx \theta_j$, $\dot{\theta}_j^2 \approx 0$.

During operation of the engine, the beam angle θ_j between the beam and the horizontal axis (e_2 for beam 1 and e_1 for beam 2)—cf. Figure 2—varies between its maximum $\theta_{j_{max}}$ and its minimum $-\theta_{j_{max}}$. Due to physical constraints of the engine, the maximum beam angle is approximately 10.21° , thus, Assumption a1 is physically correct.

3.1. Kinematics

The design of the wobble yoke mechanism is based on the classical spherical four-bar linkage [2]. These kind of linkages, which are well known in robotics, have the property that every link in the system rotates about the same fixed

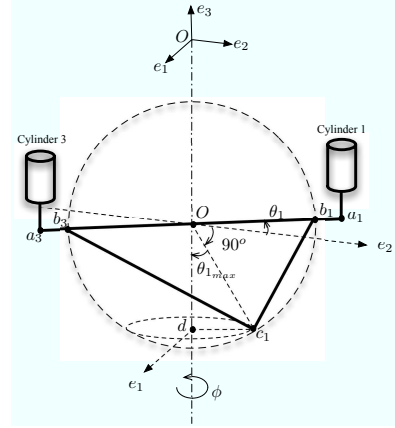


Figure 2: Schematic picture of beam 1. θ_1 is the angle between the beam and the axis e_2 , the angle ϕ is measured in the counterclockwise direction from the positive axis e_1 .

point [12, 13]. Hence, as indicated by its name, the trajectories of the points at the end of each link lie on concentric spheres. In robotics, only the revolute joint is compatible with this rotational movement and its axis must pass through the fixed point. The wobble yoke is indeed a particular class of the spherical linkage known as *spherical crank rocker* [2]. The revolute joints are replaced by the spherical bearings located at points b_1 , b_3 , c_1 and d (cf. Figure 2). The axis of the aforementioned bearings must intersect the sphere center O . Further details about spherical linkages are given in [12, 13].

Consider the schematic representation of beam 1 shown in Figure 2. We define the reference frame e_n , $n = 1, \dots, 3$, which is fixed at the pivot center of the beam O . As was explained in Section 2, the vertical motion of the pistons (not shown in Fig. 2) inside the cylinders, leads to a rotation of the beam around O . This rotation is represented by the instantaneous value of θ_1 . The variation on θ_1 causes as well a rotational movement around the axis e_3 , which is represented by the crank angle ϕ . Then, the kinematic problem for the wobble yoke Stirling engine consist in finding the equations of the angular displacements θ_j , $j = 1, \dots, 2$, and the vertical displacements z_i , $i = 1, \dots, 4$ of the connecting rod bearing center a_i , $i = 1, \dots, 4$, in terms of the crank angle ϕ .

Following the same procedure as [2], we have that—after some straightforward but cumbersome computations—the kinematic equation relating the angular displacement, velocity and acceleration θ_j , $\dot{\theta}_j$ and $\ddot{\theta}_j$ in terms of the crank angle ϕ are given respectively by¹

$$\theta = \begin{bmatrix} \theta_1 \\ \theta_2 \end{bmatrix} = \begin{bmatrix} \tan^{-1}(\kappa \sin \phi) \\ \tan^{-1}(\kappa \cos \phi) \end{bmatrix}, \quad (1)$$

$$\dot{\theta} = \begin{bmatrix} \dot{\theta}_1 \\ \dot{\theta}_2 \end{bmatrix} = \begin{bmatrix} \kappa \dot{\phi} \cos \phi \\ -\kappa \dot{\phi} \sin \phi \end{bmatrix}, \quad (2)$$

$$\ddot{\theta} = \begin{bmatrix} \kappa \ddot{\phi} \cos \phi - \kappa \dot{\phi}^2 (\sin \phi + 2 \tan^{-1}(\kappa \sin \phi) \cos^2 \phi) \\ -\kappa \ddot{\phi} \sin \phi - \kappa \dot{\phi}^2 (\cos \phi + 2 \tan^{-1}(\kappa \cos \phi) \sin^2 \phi) \end{bmatrix}, \quad (3)$$

where $\kappa = \tan \theta_{1_{max}}$. For the vertical displacements z_i , we only have two independent equations, namely, z_1 and z_2

¹Due to the lack of space, we have omitted the computation details, but we refer the reader to the companion paper [14] for the complete development of the kinematic and dynamic model.

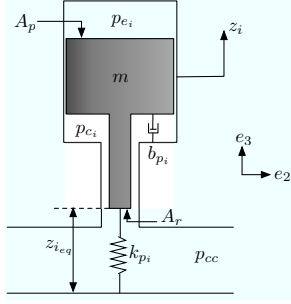


Figure 3: Free-body diagram for the pistons of the Wobble Yoke Stirling engine.

($z_3 = -z_1$ and $z_4 = -z_2$). Therefore, we define the vector $z = [z_1, z_2]^T$. Then we have

$$z = l_{Oa_1} \theta, \quad \dot{z} = l_{Oa_1} \dot{\theta}, \quad \ddot{z} = l_{Oa_1} \ddot{\theta}. \quad (4)$$

3.2. Dynamics of the Pistons Motion

In this section we borrow some inspiration from [10] to derive the motion equation of the piston depicted in Fig. 3. Consider the free-body diagram shown in Fig. 3. The dynamic equation of this system is given by

$$m\ddot{z}_i = (A_p - A_r)p_{c_i} - A_p p_{e_i} + A_r p_{cc} - k_{p_i}(z_i - z_{i_{eq}}) - b_{p_i} \dot{z}_i - mg, \quad (5)$$

where the terms $(A_p - A_r)p_{c_i}$, $A_p p_{e_i}$, and $A_r p_{cc}$ are the force in the compression space, the force in the expansion space and the force in the crank space, of the i -th cylinder, respectively. We assume that the pressure in the crank space p_{cc} is constant and equal to 1 atm.

Assume the initial condition z_{i0} to be the point of vertical static equilibrium, i.e., when the engine is not yet running, in other words, $\dot{z}_i = 0$, $\ddot{z}_i = 0$. Then the equation for the equilibrium length of the piston spring $z_{i_{eq}}$ can be obtained from (5) as follows:

$$k_{p_i} z_{i_{eq}} = -(A_p - A_r)p_{c_{i0}} + A_p p_{e_{i0}} - A_r p_{cc} + k_{p_i} z_{i0} + mg, \quad (6)$$

where $p_{c_{i0}}$ and $p_{e_{i0}}$ are the initial pressures in the compression and expansion space of the i -th cylinder, respectively. Thus, the length of $z_{i_{eq}}$ depends on the force due to the gravity and on the initial pressure difference in the cylinder. This pressure difference exists if the engine is pressurized prior to operation [10].

Substituting (6) in (5), we finally obtain the equation for the vertical motion of the i -th piston as

$$m\ddot{z}_i = (A_p - A_r)(p_{c_i} - p_{c_{i0}}) - A_p(p_{e_i} - p_{e_{i0}}) - k_{p_i}(z_i - z_{i0}) - b_{p_i} \dot{z}_i. \quad (7)$$

3.3. Thermodynamics

In the Schmidt analysis of the Stirling engine [15], the engine consist of five serially-connected components, namely, a compression space, cooler, regenerator, heater and expansion space. These five components form a thermodynamic cycle. In the case of the wobble-yoke Stirling engine, the engine is composed of four cycles (cf. Fig. 4). Each cycle consist of the compression space of cylinder i -th, the expansion space of cylinder $(i + 1)$ -th and the connecting cooler, regenerator and heater between cylinders i -th and $(i + 1)$ -th.

Since the isothermal analysis does not account for pressure gradients, we assume no pressure drop across the cooler, regenerator and heater, and thus, the pressure in the compression space of the i -th cylinder equals the pressure

in the expansion space of the adjacent cylinder $(i + 1)$ -th (cf. Fig. 4), i.e.,

$$p_{e_1} = p_{c_4}, \quad p_{e_2} = p_{c_1}, \quad p_{e_3} = p_{c_2}, \quad p_{e_4} = p_{c_3}. \quad (8)$$

By using the ideal gas law and assuming that the mass of the working gas is constant, it can be shown that the pressure variation in the compression spaces of each thermodynamic cycle is given by [15]

$$p_{c_i} = m_T R \left(\frac{V_{c_i}}{T_k} + \frac{V_k}{T_k} + \frac{V_r}{T_r} + \frac{V_h}{T_h} + \frac{V_{e_{i+1}}}{T_h} \right)^{-1} \quad (9)$$

where $T_r = (T_h - T_k) / \ln(T_h/T_k)$ is the effective temperature of the ideal regenerator assuming a linear temperature distribution.

From (9), we observe that for a given geometry, gas type and temperature distribution of the working gas, the pressure is only function of the volume variations of the compression and expansion spaces V_{c_i} and $V_{e_{i+1}}$, respectively. The volume variations depend on the piston position according to [14]

$$V_{c_i} = \frac{A_p - A_r}{2} z_i + \frac{V_{swc}}{2} + V_{dc}, \quad (10)$$

$$V_{e_i} = -\frac{A_p}{2} z_i + \frac{V_{swe}}{2} + V_{de}. \quad (11)$$

Substituting (10) and (11) into the pressure equation (9) and after grouping the constant terms in β_1 , we have that the instantaneous pressure in the compression spaces is given by

$$p_{c_i} = p_m \left(1 + \frac{A_p - A_r}{2\beta_1 T_k} z_i - \frac{A_p}{2\beta_1 T_h} z_{i+1} \right)^{-1} \quad (12)$$

where $p_m = MR/\beta_1$ is the mean pressure in the working spaces, and

$$\beta_1 = \frac{1}{T_k} \left(V_{dc} + \frac{V_{swc}}{2} \right) + \frac{1}{T_h} \left(V_{de} + \frac{V_{swe}}{2} \right) + \frac{V_k}{T_k} + \frac{V_r}{T_r} + \frac{V_h}{T_h}.$$

3.4. Rotational movement

In this section we apply a slightly modification of the approach followed by [2] to obtain the equation for the rotational movement. The main differences with [2] are the damping and spring terms in the force F_i , the computation of the equivalent forces $F_{1_{eq}}$ and $F_{2_{eq}}$ and the output shaft-torque equation τ .

We define the net forces acting at the connecting rod bearing a_i as (cf. Fig. 5)

$$F_i = m\ddot{z}_i - (A_p - A_r)(p_{c_i} - p_{c_{i0}}) + A_p(p_{e_i} - p_{e_{i0}}) + k_{p_i}(z_i - z_{i0}) + b_{p_i} \dot{z}_i. \quad (13)$$

The difference between the forces F_1 and F_3 acting at the beam ends a_1 and a_3 (cf. Fig. 5) produces an angular momentum² in the pivot center O pointing in the e_1 axis direction $M_1 = l_{Oa_1}(F_1 - F_3) - I\theta_1$. Similarly, for the second beam, we have an angular momentum in the pivot center O pointing in the e_2 axis direction $M_2 = l_{Oa_1}(F_2 - F_4) - I\theta_2$.

To get the equation of the output-shaft torque τ in the e_3 direction, we observe that the angular momenta M_1 and M_2 can be translated into equivalent forces $F_{1_{eq}}$ and $F_{2_{eq}}$ acting at the points c_1 and c_2 , for beams 1 and 2 respectively. If we constraint the forces $F_{1_{eq}}$ and $F_{2_{eq}}$ to lie in the plane $e_1 e_2$ (cf. Fig. 6), it can be shown [14] that $F_{1_{eq}} = [0, f_{1_2}, 0]^T$ and $F_{2_{eq}} = [f_{2_1}, 0, 0]^T$, with $f_{1_2} = \frac{M_1}{l_{Od}}$ and $f_{2_1} = \frac{-M_2}{l_{Od}}$. The output-shaft torque τ is then computed as (cf. Fig. 6)

$$\tau = \kappa(M_1 + M_2) \cos \phi = (M_1 + M_2) \tan \theta_2, \quad (14)$$

²Throughout the document, we follow the right-hand rule for rotational movement, i.e., a counterclockwise rotation produces a positive momentum about the rotational axis.

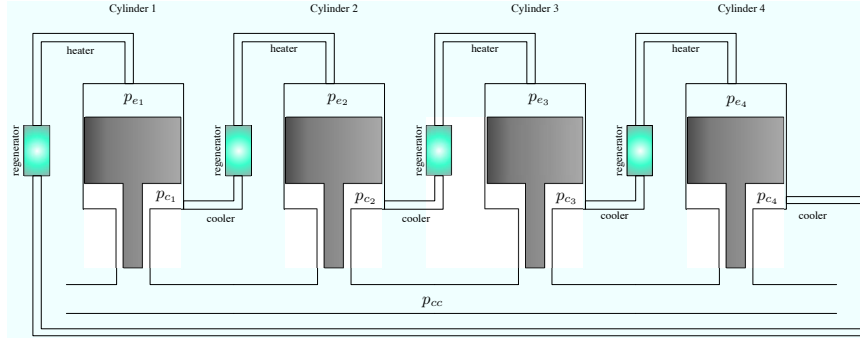


Figure 4: Thermodynamic cycles.

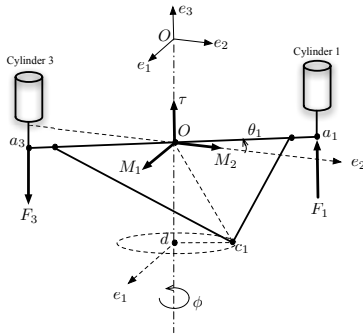


Figure 5: Forces and momenta acting on the beams

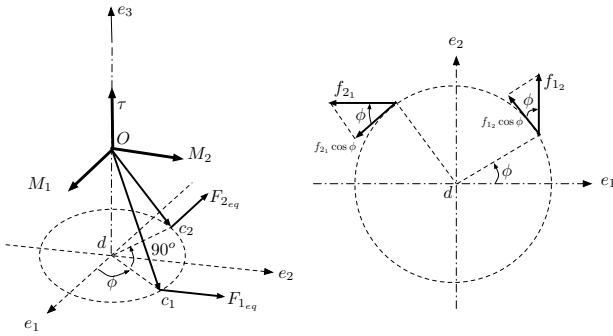


Figure 6: Equivalent forces and output-shaft-torque computation

where we have used $l_{c1d} = l_{OQ} \kappa$ and (1). By Assumption a1, $\tan \theta_2 \approx \theta_2 \approx \frac{z_2}{l_{Oa1}}$. Thus, (14) finally becomes

$$\tau = \frac{M_1 + M_2}{l_{Oa1}} z_2. \quad (15)$$

4. Conclusions and Future Work

We have developed a dynamic model of a wobble-yoke Stirling engine mechanism with a four-cylinder double-acting configuration. Because of the pressure dynamics (12), the piston motion equation (7) are nonlinear. However, the system can be studied via linear analysis methods due to the linear spring behavior of the working gas [16]. Current research is underway to validate and investigate the stability properties of the model. See [14] for further details.

Among the issues that are currently being explored are the application of the wobble-yoke Stirling engine in

micro-CHP systems, particularly, those composed of an electricity generator driven by the wobble-yoke Stirling engine.

References

- [1] D. M. Clucas and J. K. Raine. Development of a hermetically sealed stirling engine battery charger. In *Proc. of the Institution of Mechanical Engineers, IMechC*, volume 208, pages 357–366, Jan 1994.
- [2] D. M. Clucas and J. K. Raine. A new wobble drive with particular application in a Stirling engine. In *Proc. of the Institution of Mechanical Engineers, IMechE*, volume 208, pages 337–346, 1994.
- [3] G. Smith and S. Barnes. Electrical power generation from heat engines. *Power Electronics for Renewable Energy (Digest No: 1997/170), IEE Colloquium on*, 170:5/1 – 5/6, May 1997.
- [4] J. Harrison. Micro combined heat and power (CHP) for housing. In *SET 2004–3rd. Conference on Sustainable Energy Technologies*, Nottingham, UK., Jun 28–30 2004.
- [5] H. Onovwiona and V. Ugursal. Residential cogeneration systems: review of the current technology. *Renewable and Sustainable Energy Reviews*, 10:389–431, Jan 2006.
- [6] R. W. Redlich and D. M. Berchowitz. Linear dynamics of a free-piston Stirling engines. In *Proc. of the Institution of Mechanical Engineers, IMechE*, volume 199, pages 203–213, 1985.
- [7] M. Kankam and J. Rauch. Controllability of free-piston Stirling engine/linear alternator driving a dynamic load. In *28th Intersociety Energy Conversion Engineering Conference*, Atlanta, Georgia, Aug 8–13 1993. ANS, SAE, ACS, IEEE, ASME, AIAA, AIChE.
- [8] I. Burrell, S. Leballois, E. Monmasson, and L. Prevond. Energy performance and stability of Stirling micro-cogeneration system. In *Power Electronics and Motion Control Conference 2006, EPE-PEMC*, pages 2057 – 2063, Portoroz, Slovenia, Aug 2006.
- [9] G. Benvenuto and F. de Monte. Analysis of free-piston Stirling engine/linear alternator systems: Part 1: Theory, part ii: Results. *Journal of Propulsion and Power*, 11(5):1036–1055, October 1995.
- [10] J. Riefrio, K. Al-Dakkan, M. Hofacker, and E. Barth. Control-based design of free-piston Stirling engines. In *American Control Conference 2008*, pages 1533 – 1538, Seattle, Washington, USA, May 2008.
- [11] Whispergen heat and power systems. <http://www.whispergen.com>.
- [12] C. H. Chiang. *Kinematics of spherical mechanisms*. Cambridge University Press, (Cambridge [England], New York), 1988.
- [13] J. Michael McCarthy. *Geometric Design of Linkages*. Springer, 1 edition, April 2000.
- [14] E. García-Canseco and J. M. A. Scherpen. Modeling for control of a wobble yoke stirling engine. Internal report, 2009.
- [15] I. Urierli and D. M. Berchowitz. *Stirling Cycle Engine Analysis*. Adam Hilger Ltd, Bristol, 1984.
- [16] M. D. Kankam and J. S. Rauch. Comparative survey of dynamic analyses of free-piston Stirling engines. In *26th Intersociety Energy Conversion Engineering Conference*, Boston, Massachusetts, August 4–9 1991.